Effect of Charge-Modulated Molecular Passivator on Methylammonium/Bromine-Free Inverted Perovskite Solar Cells

Dhruba B. Khadka[1], Yasuhiro Shirai[1], Masatoshi Yanagida[1] and Kenjiro Miyano[1]

[1]Photovoltaics Materials Group, Global Research Center for Environment and Energy based on Nanomaterials Science (GREEN), National Institute for Materials Science (NIMS), 1-1 Namiki, Tsukuba, Ibaraki 305-0044, Japan

***Abstract* — This study explores the potential of molecular passivation to enhance both the efficiency and operational stability of perovskite solar cells. We investigate the impact of diammonium iodide functional molecules with aryl or alkyl cores on 3D-perovskite surfaces. We found that piperazine dihydriodide, featuring an alkyl core and an electron-rich -NH terminal was effective in mitigating surface and bulk defects. This molecular passivator not only modifies surface chemistry but also improves carrier extraction efficiency, leading to an impressive 23.17% efficiency with superior long-term stability. Detailed device analysis suggests that robust bonding interactions significantly reduce defect densities in the perovskite film and suppress ion migration. This report provides insights into the synergistic effect of bifunctional molecules in defect mitigation, paving the way for design strategies centered on bonding-regulated molecular passivation to enhance both the performance and stability of solar cells.**

I. Introduction

Perovskite solar cells (PSCs) demonstrated conversion efficiency (PCE) of over 26.1%, approaching to Shockley–Queisser limit.[1], [2] However, perovskite films are still prone to degradation under external factors and intrinsic phenomena.[3]–[5] To address these detrimental defect chemistries, molecular passivation has been of great interest in improving the PCE and device stability.[6]

Recently, MA-free formamidinium (FA)-based HP has garnered significant attention due to its higher thermal stability, moisture resistance, and better absorbance in the near-infrared region.[7] Alkali or organic cations have been introduced into the FA-perovskite film to promote the growth of the photoactive black phase at low-temperature crystallization.[8], [9] For example, alloyed FA-perovskite with organic cation has demonstrated an impressive PCE of 24.4% in the normal device configuration.[10] In addition, some reports have focused on the versatile molecular passivation strategy aimed at mitigating various intrinsic point defects in the HP film.[2] They have used multifunctional derivatives consisting of amine,[11] Lewis acids/bases,[12], [13] supramolecules,[14], [15] ionic polymer,[16] for mitigation of defect chemistry in the HPSCs.

This report presents a passivation strategy through bond/charge regulated defect passivation by introducing bifunctional molecules with an aryl core (1,4-phenylenediamine dihydrodide (PEDAI)) or alkyl core (piperazine dihydriodide (PZDI)) onto the MA-free HP film in inverted PSCs. We demonstrate that the different molecular properties lead to distinct differences in the film growth, material distribution, and device characteristics. The PSCs with PZDI treatment resulted in an enhanced large area (>1cm^2) device performance from 19.68 to 23.17% (inverted configuration) with superior device stability under thermal and moisture stress.

II. Detailed Text Formatting

A. Device fabrication

For the fabrication of MA-free HP of composition-$FA_{0.84}Cs_{0.12}Rb_{0.04}PbI_3$: the precursor solution (1.05 M) was prepared by dissolving FAI (0.84 M), CsI (0.12 M), RbI (0.04 M), PbI_2 (1 M), and 5-AVAI (1 mM) in the mixture of dimethylformamide and dimethyl sulfoxide (4:1) solvent for 2 hours. The sputtered NiO_x thin film was treated with MeO-2PACz.[15], [17] For film deposition, the precursor was spin-coated at 1000 rpm-10 s and 5000 rpm-40 s followed by dripping 800 µl of CB at 34th s of the 2nd step. Then, these as-grown films were simply placed on a hot plate at 60℃ for 1 min and at 100℃ for 45 min. For surface passivation, PEDAI and PZDI precursor solutions of different concentrations (0.5 – 3 mg/ml) were spin-coated onto the HaP film at 5000 rpm-40 s and annealed at 100℃-5 min. Then, we deposited C_{60} and BCP by thermal evaporation. Finally, Ag was thermally evaporated. The details have been discussed in our earlier reports.[18]–[21]

B. Materials and device characterizations

XRD data were measured using Rigaku Smart Lab, CuKα radiation, λ=1.5405Å. Scanning electron microscopy (SEM) images were collected by a high-resolution scanning electron microscope (SEM) at 5 kV accelerating voltage (Hitachi, S-4800). The absorption and photoluminescence (PL) spectra were measured using a micro-PL spectrometer (HORIBA, LabRamHR-PL NF(UV-NIR). The current density–voltage (J-V) curves were measured under 1 sun with an AM1.5G spectral filter coupled with an MPPT system (Systemhouse Sunrise Corp.). Capacitance spectra (C–f) were collected using an LCR meter (IM3536, Hioki) in the dark.

III. Results and Discussion

To examine the photovoltaic effect of molecular treatment, PSC and its characteristics have been investigated. The molecules used for surface passivation are given in Fig. 1a,c. These molecules show distinct characteristics in terms of bond length and Mulliken charge distribution that could be useful for effectively suppressing charge defects in the perovskite film. The device structure is as depicted in Fig. 1b.

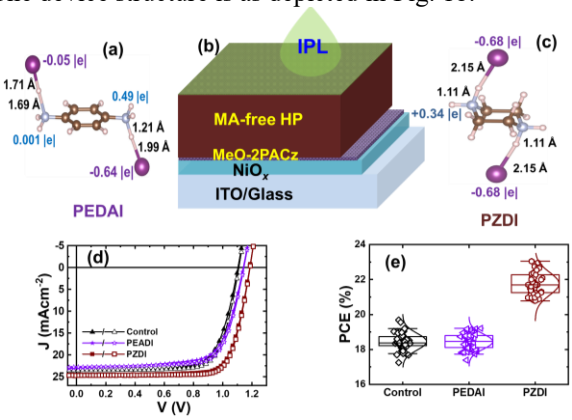

Figure 1. Molecular structure of surface charge surface passivators (a) PEDAI and (c) PZDI and (b) schematic of molecular passivation. J-V curves of Pb-PSCs with surface treatments (d). Statistics of device efficiency trend (e).

To explore the effect of surface treatment using PEDAI or PZDI on the photovoltaic properties, PSCs with inverted device structures were fabricated. Figure 1d displays current density-voltage (J-V) curves of the control and PEDAI or PZDI passivated PSCs. The control device yields a PCE of 19.6%. The PZDI-treated PSC demonstrates a superior PCE of 23.2% (V_{OC}=1.188 V, FF=0.787, J_{SC}=24.78 mA/cm^2) compared to PEDAI treated device (PCE=19.21%;V_{OC}=1.145 V, FF=0.736, J_{SC}=22.79 mA/cm^2). All of the J-V curves have negligible hysteresis. As we compare the surface passivator, PEDAI has a delocalized lone pair of electrons of nitrogen atoms while that in PZDI is localized. The nitrogen site in DIM enhances the surface adhesion on the HP film which is favorable for defect mitigation. Hence, PZDI-treated PSC has much higher device performance. The PCE statistics are displayed in Fig. 1e. We validated PSCs with MA/Br-free HP film with PZDI treatment of PCE ≈21.47% (area ≈1.024 cm^2) under standard conditions (accredited independent photovoltaic test laboratory, AIST PV Lab, Japan).

Figures 2a-c display the surface morphology of MA/Br-free HP film (control, with PEDAI or PZDI). It shows a slight change in the grain size with an overlayer surface on the film. The HP film with PEDAI passivation grows with unevenly distributed small crystallite while the HP film with PZDI treatment forms well-covered surface and grain boundaries which is beneficial for passivation of surface defect and interface quality.

Figures 2d,e show XRD patterns of control, perovskite films with PEDAI or PZDI surface treatment, mixed in perovskite and PbI_2 film. The PZDI-treated HP films show a dominant (110) characteristic diffraction peak of the α-phase of FA- HP. It suppresses the δ-Cs/RbPbI3 phase and residual PbI_2. The characteristic XRD peak at lower 2θ on the HP film with PEDAI treatment grows with higher intensity indicating higher tendency for the formation of 2D phase compared to alkyl counterpart.

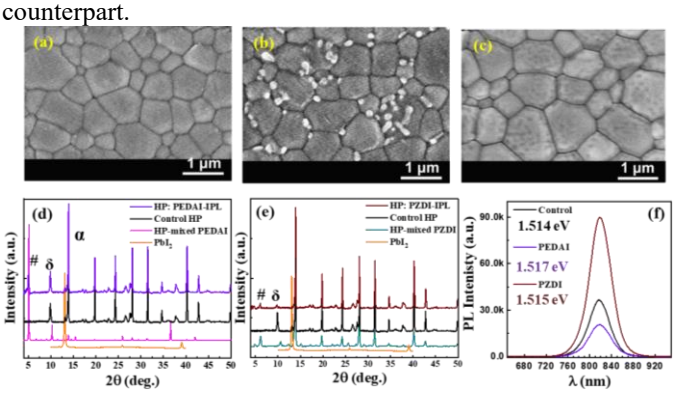

Fig. 2. Effect of surface treatment: SEM image of surface treatment-(a) control, (b) PEDAI, (c) PZDI. XRD patterns (d, e) (#-2D phase, δ-non-photoactive perovskite phase and (f) PL spectra of HP film: control, PEDAI, and PZDI treatment.

The PL spectra of respective films are given in Fig. 2f. The PZDI-treated film demonstrates an intensified peak while the PEDAI-treated film has suppressed compared to the control film. It shows a minimal shifting of the PL characteristic peak (~817-818 nm; bandgap listed in inset) suggesting no incorporation of PEDAI or PZDI into the 3D-HP lattice. It is also consistent with XRD patterns.

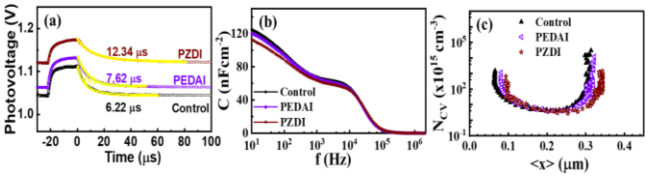

Fig. 3. Device characteristics: TPV spectra (a), C-f spectra at room temperature (b), and carrier profile extracted from capacitance spectra (c).

Transient photovoltage (TPV) responses are displayed in Figure 3a. The PZDI-treated device (12.34 μs) reveals a longer carrier lifetime compared to PEDAI (7.62 μs) and the control device (6.22 μs). It indicates that the PZDI treatment passivates the defect in the HP film.

We also measure the capacitance spectra of respective devices to explore the defect properties. Figure 3b gives the capacitance-frequency (C-f) spectra of all devices. PZDI-treated PSC shows a plateau regime (1 to 100 kHz) with a slightly lower value accounting for lower defect density. Furthermore, the carrier profile (N_{CV}) (Figure 3c) extracted from C-V data analysis showed a carrier distribution in a bulk in the range of ~3.46-6.94 ×10^{15} cm^{-3}. The N_{CV} with PZDI is slightly lower by some fraction. The carrier profile at the edge

accounts for the interface defect density. It is found to be suppressed by 6 times for the PZDI-device suggesting attenuation of the recombination activities.

IV. SUMMARY AND CONCLUSIONS

This work presents interfacial passivation on 3D-HaP using charge-modulated molecular passivation (PEDAI or PZDI) for the fabrication of the inverted PSCs with sputtered NiOx as HTL with SAM layer. It enhanced PCE from ~19.65 to 23.17% using PZDI, alkyl core amine derivatives. The PZDI molecules with alkyl core are found to be beneficial for the improvement in film quality by quenching the surface and bulk defect due to stronger interaction with localized electron density. This report highlights a new way of designing molecular passivation with charge-regulated molecular bonding for efficient and stable PSC.

ACKNOWLEDGMENT

This work was supported by JST-Mirai Program Grant Number JPMJMI21E6, Japan.

REFERENCES

[1] O. Almora *et al.*, 'Device Performance of Emerging Photovoltaic Materials (Version 3)', *Adv Energy Mater*, vol. 13, no. 1, p. 2203313, Jan. 2023, doi: 10.1002/aenm.202203313.

[2] D. B. Khadka *et al.*, 'Advancing Efficiency and Stability of Lead, Tin, and Lead/Tin Perovskite Solar Cells: Strategies and Perspectives', *Solar RRL*, Aug. 2023, doi: 10.1002/solr.202300535.

[3] D. B. Khadka, Y. Shirai, M. Yanagida, K. Uto, and K. Miyano, 'Analysis of degradation kinetics of halide perovskite solar cells induced by light and heat stress', *Solar Energy Materials and Solar Cells*, vol. 246, p. 111899, Oct. 2022, doi: 10.1016/j.solmat.2022.111899.

[4] D. B. Khadka, Y. Shirai, M. Yanagida, and K. Miyano, 'Degradation of encapsulated perovskite solar cells driven by deep trap states and interfacial deterioration', *J Mater Chem C Mater*, vol. 6, no. 1, pp. 162–170, 2018, doi: 10.1039/C7TC03733C.

[5] I. Gueye *et al.*, 'Analysis of Iodide Transport on Methyl Ammonium Lead Iodide Perovskite Solar Cell Structure Through Operando Hard X-ray Photoelectron Spectroscopy', *Chemistry of Materials*, vol. 35, no. 5, pp. 1948–1960, Mar. 2023, doi: 10.1021/acs.chemmater.2c03162.

[6] Y. Liu *et al.*, 'Ultrahydrophobic 3D/2D fluoroarene bilayer-based water-resistant perovskite solar cells with efficiencies exceeding 22%', *Sci Adv*, vol. 5, no. 6, p. eaaw2543, Jun. 2019, doi: 10.1126/sciadv.aaw2543.

[7] J. Lee, D. Seol, A. Cho, and N. Park, 'High-Efficiency Perovskite Solar Cells Based on the Black Polymorph of $HC(NH_2)_2PbI_3$', *Advanced Materials*, vol. 26, no. 29, pp. 4991–4998, Aug. 2014, doi: 10.1002/adma.201401137.

[8] S.-H. Turren-Cruz, A. Hagfeldt, and M. Saliba, 'Methylammonium-free, high-performance, and stable perovskite solar cells on a planar architecture', *Science (1979)*, vol. 362, no. 6413, pp. 449–453, Oct. 2018, doi: 10.1126/science.aat3583.

[9] D. B. Khadka, Y. Shirai, M. Yanagida, and K. Miyano, 'Attenuating the defect activities with a rubidium additive for efficient and stable Sn-based halide perovskite solar cells', *J Mater Chem C Mater*, vol. 8, no. 7, pp. 2307–2313, 2020, doi: 10.1039/C9TC06206H.

[10] G. Kim, H. Min, K. S. Lee, D. Y. Lee, S. M. Yoon, and S. Il Seok, 'Impact of strain relaxation on performance of a-formamidinium lead iodide perovskite solar cells', *Science (1979)*, vol. 370, no. 6512, pp. 108–112, Oct. 2020, doi: 10.1126/science.abc4417.

[11] D. B. Khadka, Y. Shirai, M. Yanagida, and K. Miyano, 'Pseudohalide Functional Additives in Tin Halide Perovskite for Efficient and Stable Pb-Free Perovskite Solar Cells', *ACS Appl Energy Mater*, vol. 4, no. 11, pp. 12819–12826, Nov. 2021, doi: 10.1021/acsaem.1c02496.

[12] T. Li *et al.*, 'Multiple functional groups synergistically improve the performance of inverted planar perovskite solar cells', *Nano Energy*, vol. 82, p. 105742, Apr. 2021, doi: 10.1016/j.nanoen.2021.105742.

[13] D. B. Khadka, Y. Shirai, M. Yanagida, T. Tadano, and K. Miyano, 'Alleviating Defect and Oxidation in Tin Perovskite Solar Cells Using a Bidentate Ligand', *Chemistry of Materials*, vol. 35, no. 11, pp. 4250–4258, Jun. 2023, doi: 10.1021/acs.chemmater.3c00243.

[14] A. Abate *et al.*, 'Supramolecular Halogen Bond Passivation of Organic–Inorganic Halide Perovskite Solar Cells', *Nano Lett*, vol. 14, no. 6, pp. 3247–3254, Jun. 2014, doi: 10.1021/nl500627x.

[15] D. B. Khadka, Y. Shirai, M. Yanagida, T. Tadano, and K. Miyano, 'Interfacial Embedding for High-Efficiency and Stable Methylammonium-Free Perovskite Solar Cells with Fluoroarene Hydrazine', *Adv Energy Mater*, vol. 12, no. 38, p. 2202029, Oct. 2022, doi: 10.1002/aenm.202202029.

[16] S. Bai *et al.*, 'Planar perovskite solar cells with long-term stability using ionic liquid additives', *Nature*, vol. 571, no. 7764, pp. 245–250, Jul. 2019, doi: 10.1038/s41586-019-1357-2.

[17] M. Yanagida, T. Nakamura, T. Yoshida, D. B. Khadka, Y. Shirai, and K. Miyano, 'Surface modification of sputtered NiOx hole transport layer for CH3NH3PbI3perovskite solar cells', *Jpn J Appl Phys*, vol. 62, no. SK, p. SK1054, Aug. 2023, doi: 10.35848/1347-4065/acd5dc.

[18] D. B. Khadka, Y. Shirai, M. Yanagida, T. Masuda, and K. Miyano, 'Enhancement in efficiency and optoelectronic quality of perovskite thin films annealed in MACl vapor', *Sustain Energy Fuels*, vol. 1, no. 4, pp. 755–766, 2017, doi: 10.1039/C7SE00033B.

[19] D. B. Khadka, Y. Shirai, M. Yanagida, J. W. Ryan, and K. Miyano, 'Exploring the effects of interfacial carrier transport layers on device performance and optoelectronic properties of planar perovskite solar cells', *J Mater Chem C Mater*, vol. 5, no. 34, pp. 8819–8827, 2017, doi: 10.1039/C7TC02822A.

[20] D. B. Khadka, Y. Shirai, M. Yanagida, T. Noda, and K. Miyano, 'Tailoring the Open-Circuit Voltage Deficit of Wide-Band-Gap Perovskite Solar Cells Using Alkyl Chain-Substituted Fullerene Derivatives', *ACS Appl Mater Interfaces*, vol. 10, no. 26, pp. 22074–22082, 2018, doi: 10.1021/acsami.8b04439.

[21] D. B. Khadka, Y. Shirai, M. Yanagida, and K. Miyano, 'Unraveling the Impacts Induced by Organic and Inorganic Hole Transport Layers in Inverted Halide Perovskite Solar Cells', *ACS Appl Mater Interfaces*, vol. 11, no. 7, pp. 7055–7065, Feb. 2019, doi: 10.1021/acsami.8b20924.